Roughness effects on magnetic properties of thin films

Palasantzas, G.; Zhao, Y.P.; de Hosson, J.T.M.; Wang, G.C.

Published in:
Physica B: Condensed Matter

DOI:
10.1016/S0921-4526(99)01939-0

Publication date:
2000

ELSEVIER

Physica B 283 (2000) 199–202

PHYSICA B

www.elsevier.com/locate/physb

Roughness effects on magnetic properties of thin films

G. Palasantzas[a,*], Y.-P. Zhao[b], J.Th.M. De Hosson[a], G.-C. Wang[b]

[a]*Department of Applied Physics and Materials Science Center, Netherlands Institute for Metals Research, University of Groningen, Nijenborgh 4, 9747 AG Groningen, The Netherlands*

[b]*Department of Physics, Applied Physics, and Astronomy, and Center for Integrated Electronics and Electronics Manufacturing, Rensselaer Polytechnic Institute, Troy, NY 12180-3590, USA*

Abstract

X-ray and electron diffraction have been used to determine the surface roughness parameters of thin films and thus evaluate roughness effects on magnetic properties. For self-affine roughness, the demagnetizing factor is influenced by the roughness exponent H, and is proportional to w/ξ^2 with w being the RMS roughness amplitude and ξ being the lateral correlation length. Roughness anisotropy can amplify in-plane demagnetising factors. Roughness can also influence the coercivity through the RMS local surface slope.

Keywords: Magnetic films; Magnetic properties; Surface/interface scattering; Surface roughness

1. Introduction

Surface and interface roughness influence magnetic anisotropy, coercivity, magnetic domain structure, magnetoresistance, etc. [1]. For NiFeCo films the coercivity increased with increasing surface roughness [2]. For Co films deposited on plasma etched Si(100) substrates, the uniaxial anistropy decreased and disappeared for the roughest films. Also, the magnetization reversal mechanism was strongly influenced by roughness [3]. For ultrathin Co film deposited on rough Cu(001) substrates, the coercivity was higher than that deposited on a smooth Cu(001) substrate [4]. X-ray and high-resolution–low-energy-electron diffraction (HRLEED) techniques [5–8] have been used for measuring surface/interface roughness parameters quantitatively. These parameters are then used to analyse roughness contributions on magnetic properties of thin films. In this work we will focus on roughness effects on the demagnetising factor and coercivity of thin magnetic films.

2. Roughness effects on demagnetizing factor and coercivity

2.1. Demagnetizing factor

In general, the demagnetizing field of a magnetic film is caused by magnetic poles generated near film boundaries due to its finite shape which oppose the applied field. We denote $\boldsymbol{M}$ and $\boldsymbol{N}$ as the uniform film magnetization and demagnetizing tensor, respectively [9,10]. For a film of thickness d with substrate/film/vacuum rough boundaries at growth front $-d/2 + h_2(\boldsymbol{r})$ and substate $d/2 + h_1(\boldsymbol{r})$ ($\langle h_i(\boldsymbol{r})\rangle = 0$, $i = 1,2$), the in-plane components of $\boldsymbol{N}$ are given by (for $|h_i(\boldsymbol{r})| \ll d$, $i = 1,2$) [9,10]

$$N_{xx(yy)} = \frac{(2\pi)^4}{2\mathrm{d}A}\int_{0<k<Q_c}(k^2_{x(y)}/k)\left[\sum_{i=1}^{2}\langle|h_i(\boldsymbol{k})|^2\rangle - 2\mathrm{e}^{-\mathrm{d}k}\langle h_1(\boldsymbol{k})h_2(-\boldsymbol{k})\rangle\right]\mathrm{d}\boldsymbol{k}, \quad (1)$$

where $h_i(\boldsymbol{k})$ is the Fourier transform of $h_i(\boldsymbol{r})$. Here A is the area of a surface, and Q_c is the high spatial frequency cutoff. Finally, $N_{zz} = 1 - N_{xx} - N_{yy}$ while $N_{xy} = N_{xz} = 0$ to first-order upon an ensemble average [9,10].

* Corresponding author.
E-mail address: g.palasantzas@phys.rug.nl (G. Palasantzas)

0921-4526/00/$ - see front matter
PII: S0921-4526(99)01939-0

2.2. Coercivity

We denote H_c as the coercive field and δ the domain wall width. Following Soohoo and Middelhoek [11,12], we treat the coercivity H_c for a single rough boundary and a straight wall moving parallel to itself as [13,14]

$$H_c = \frac{1}{2M}\left\{\frac{\partial E_w}{\partial d} + \frac{E_w}{d}\right\}\rho_{rms};$$

$$\rho_{rms} = \left\{\frac{(2\pi)^4}{A}\int_{Q_\delta}^{Q_c} k^2\langle|h(\boldsymbol{k})|^2\rangle \mathrm{d}\boldsymbol{k}\right\}^{1/2}, \quad (2)$$

where the domain energy is E_w and the thickness fluctuations are represented by the local surface slope $\rho_{rms} = \sqrt{\langle \nabla h^2\rangle}$ [15,16]. $Q_c = \pi/a_0$ with a_0 being the order of an atomic spacing, and $Q_\delta = 2\pi/\delta$. For a Neel wall, $E_w = A_{ex}(\pi^2/\delta)K_{in}(\delta/2) + \pi M^2\,\mathrm{d}\delta/(\mathrm{d}+\delta)$. $A_{ex} = JS^2/a_e$ is the exchange constant ($J = 155$ K and a_e is an atomic length scale), and S the average spin (< 0.65 for $d < 10$ nm) [8]. $K_{in} = K_v + (2K_s/d)$ is the in-plane anisotropy constant with K_v and K_s being the in-plane volume and surface anisotropy constants, respectively [11,12].

3. Roughness models

Our calculations or roughness effects are performed for self-affine rough surfaces observed in magnetic films [3,4,17] and rough growth fronts based on linear Langevin equations [18].

3.1. Roughness for self-affine fronts

Isotropic self-affine roughness is characterized by the RMS roughness amplitude w, the lateral in-pnane correlation length ξ, and the roughness exponent $H(0 < H < 1)$ which characterize the degree of surface irregularity at short roughness wavelengths ($< \xi$) [5–8,17]. A simple self-affine model in Fourier space [15,16] reads of the form

$$\langle|h(\boldsymbol{k})|^2\rangle = \frac{A}{(2\pi)^5}\frac{w^2\xi^2}{(1 + ak^2\xi^2)^{1+H}};$$

$$a = \frac{1}{2H}\left[1 - (1 + aQ_c^2\xi^2)^{-H}\right], \quad (3)$$

which will be used to calculate the demagnetizing factor and coercivity (Eqs. (1) and (2)).

3.2. Roughness for linear growth fronts

Stable linear growth fronts [18] are described by Langevin equations $\partial h(\boldsymbol{r},t)/\partial t = v\nabla^2 h(\boldsymbol{r},t) - K\nabla^4 h(\boldsymbol{r},t) + \eta(\boldsymbol{r},t)$ with $\eta(\boldsymbol{r},t)$ being a Gaussian noise of amplitude D. The parameter κ is proportional to the surface diffusion coefficient, and v is proportional to surface tension which is the result of the evaporation/recondensation process. Solution of this linear equation yields [18]

$$\langle|h_2(\boldsymbol{k},t)|^2\rangle = \mathrm{e}^{2L(k)t}\langle|h_1(\boldsymbol{k},t)|^2\rangle + (4\pi)[A/(2\pi)^5] \times D(\mathrm{e}^{2L(k)t} - 1)L(k)^{-1}. \quad (4)$$

$$\langle h_1(\boldsymbol{k},t)h_2(-\boldsymbol{k},t)\rangle = \mathrm{e}^{2L(k)t}\langle|h_1(\boldsymbol{k},t)|^2\rangle,$$

$$L(k) = -vk^2 - \kappa k^4.$$

For $v > 0$ and $\kappa = 0$ we obtain $H = 0$, while for $v = 0$ and $\kappa > 0$ we have $H = 1$. For $v < 0$, Eq. (4) describes intitial stages of unstable growing surfaces [18].

4. Results and discussions

4.1. Demagnetizing factor

For simplicity, we will present results mainly for films with a single rough boundary. As shown in Fig. 1(a), for a self-affine surface, $N_{xx(yy)}$ is strongly affected by the

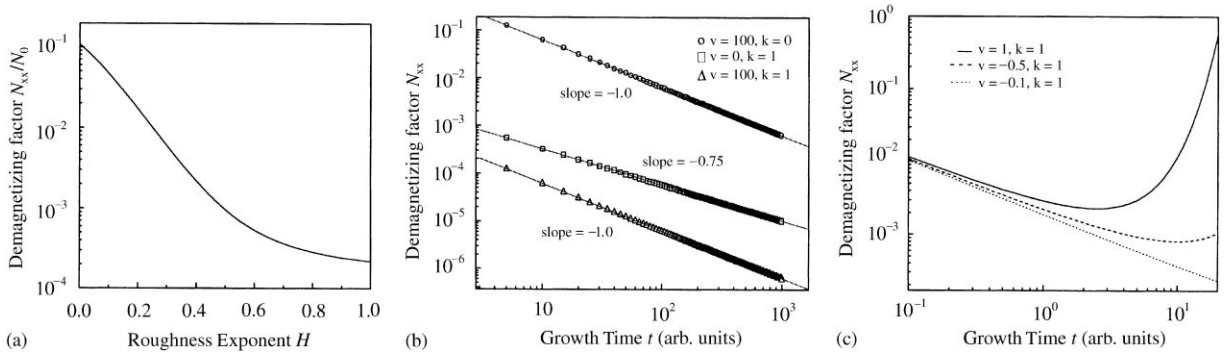

Fig. 1. (a) N_{xx} versus H for $d = 90$ nm, $\xi = 200$ nm and $w = 1$ nm. (b) N_{xx} versus growth time t with $F/D = 200$ and F the average deposition rate ($d = Ft$). (c) N_{xx} versus t for unstable growth.

roughness exponent H and to a leading order is proportional to w/ξ^2 [15–17]. Extending Eq. (3) for surfaces with correlation length anisotropy $\langle|h(\boldsymbol{k})|^2\rangle \propto \xi_x\xi_y/(1+k_x^2\xi_x^2+k_y^2\xi_y^2)^{1+H}$, it can be shown that $N_{xx}/N_{yy} \propto (\xi_y/\xi_x)^c$ where $c=1.7$ [9,10] suggesting that roughness anisotropy can amplify the demagnetizing factors drastically.

We also examine the evolution of $N_{xx(yy)}$ with thickness or alternatively growth time t for films grown on a smooth substrate ($h_1=0$) with linear mechanism. Fig. 1(b) indicates that $N_{xx(yy)}$ scales as $N_{xx(yy)} \propto t^{-\varepsilon}$ with $\varepsilon \approx 2\beta - \beta/H - 1$. β is the growth exponent such that $w \propto t^{\beta}$ and $\xi \propto t^{H/\beta}$ [5–8,17]. For $v=0$ and $\kappa=1$ we obtain numerically $\varepsilon=0.75$, while the model solution yields the consistent result $\varepsilon \approx 2\beta - \beta/H - 1 = 3/4$ ($H=1, \beta=1/4$). For $v=100$ and $\kappa=0$, $N_{xx(yy)}$ is larger than for $v=0$ and $\kappa=1$, since the former corresponds to $H=0$ and the later corresponds to $H=1$ [5–8,17]. For $v<0$ (unstable growth; Schowebel barrier effect) [18] a drastic increase of $N_{xx(yy)}$ occurs at later stages of growth due to strong roughening, see Fig. 1(c).

4.2. Coercivity

For the Co films deposited on Cu(001), the roughness parameters w, H, and ξ were determined by HRLEED [4]. Fig. 2 shows $\rho_{\rm rms}$ d (arrow pointing on the left), where roughening of the Co films is evident since $\rho_{\rm rms}$ increases almost one order of magnitude for $2 \leqslant d \leqslant 25$ ML. Experimentally, H_c increased up to ~ 80 Oe at d–7 ML, and then slightly decreased and approached saturation [4]. Using $K_v = -2.3\times10^6$ erg/cm^3, $a_e = 0.25$ nm [11,12], $S=0.05$, $K_s = 0.034$ erg/cm^2, $M_s = 1400$ emu, and wall thickness δ–5 nm [13,14], H_c can be calculated as shown in Fig. 2 (arrow pointing on the right). For an FCC lattice (which is close to the FCT Co/Cu(001) growth lattice), the variation of M with film thickness d is given by [19]

$$M(d)/M_s = 1 - (k_B T/16\pi S^2 G_3 J) f(d), f(d) = \sum_{\lambda_3=1}^{3} C_3[\ln(1-e^{-B}) - \ln(1-e^{-A})],$$

$$A = (16JS/k_B T)[\{1-\pi^2/4G^2\} - \{1+\pi^2/4G^2\}\cos k_3],$$

$$B = (16JS/k_B T)[\{1-\pi/4\} - \{1+\pi/4\}\cos k_3],$$

$$C_3 = (1+\cos k_3)^{-1} \quad (5)$$

with $G_3 = d/a_o$, $k_3 = 2\pi\lambda_3/G_3$ and $G \geqslant 10^7$. The calculated coersivity at ~ 15 ML is close to the experimental data for the Co [4] films, ~ 120 Oe, and decreases slightly for further increase of the film thickness, see Fig. 2.

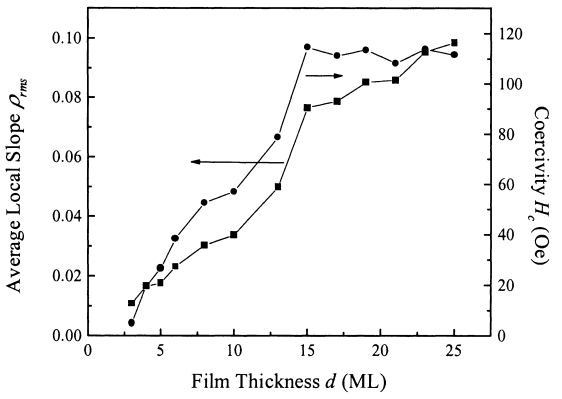

Fig. 2. Average local slope $\rho_{\rm rms}$ (squares; calculated from the experimental data in Ref. [4].) and coercivity H_c (circles) versus thickness d for Co films deposited on Cu(001).

5. Conclusions

Surface/interface roughness and thin film growth mechanisms can have strong influence on magnetic properties of thin films. Therefore, a precise determination of film roughness as well as its growth mechanism using X-ray and electron diffraction stands as a necessary step to correlate microstructural disorder with magnetic properties. We have worked out theoretically that the knowledge of demagnetizing factor $N_{xx(yy)}$ allows more precise determination of roughness effects on coercivity, domain wall width, and domain sizes.

Acknowledgements

Work at Rensselaer Polytechnic Institute was supported by NSF.

References

[1] J.A.C. Bland, B. Heinrich (Eds.), Ultrathin Magnetic Structures I and II, Springer, New York, 1994.
[2] V.I. Malyutin et al., Phys Status Solid A 65 (1981) 45.
[3] M. Li, G.-C. Wang, H.-G. Min, J. Appl. Phys. 83 (1998) 5313.
[4] Q. Jiang, H.-N. Yang, G.-C. Wang, Surf. Sci. 373 (1997) 181.
[5] S.K. Sinha et al., Phys. Rev. B 38 (1988) 2297.
[6] V. Holy et al., Phys. Rev. B 47 (1993) 15 896.
[7] D.K.G. de Boer, Phys. Rev. B 53 (1996) 6048.
[8] H.-N. Yang, G.-C. Wang, T.-M. Lu, Diffraction from Rough Surfaces and Dynamic Growth Fronts, World Scientific, Singapore, 1993.
[9] Y.-P. Zhao, G. Palasantzas, G.-C. Wang, J.Th.M. De Hosson, Phys. Rev. B 60 (1999) 1216.
[10] G. Palasantzas, J. Appl. Phys. 86 (1999) 2196.
[11] R.F. Soohoo, J. Appl. Phys. 52 (1981) 2461.

[12] G. Drukerij Wed, N.V. Van Soest, S. Middelhoeok, (Eds.), Ferromagnetic Domains in Thin Ni–Fe Films, Amsterdam, 1961.
[13] Y.-P. Zhao, G. Palasantzas, G.-C. Wang, J.Th.M. De Hosson, in preparation.
[14] G. Palasantzas, Phys. Rev. E 56 (1997) 1254.
[15] G. Palasantzas, Phys. Rev. B 48 (1993) 14 472.
[16] G. Palasantzas, Phys. Rev. B 49 (1994) E5785.
[17] J. Krim, G. Palasantzas, Int. J. Mod. Phys. B 9 (1995) 599.
[18] Y.-P. Zhao, H.-Y. Yang, G.-C. Wang, T.-M. Lu, Phys. Rev. B 57 (1998) 1922.
[19] S.J. Glass, M.J. Klein, Phys. Rev. 109 (1958) 288.